Electronic Supplementary Material (ESI) for CrystEngComm.
This journal is © The Royal Society of Chemistry 2017

Supporting Information

Hetero-epitaxial Growth Control of Single-crystalline Anatase TiO_2 Nanosheets Predominantly Exposing the {001} Facet on Oriented Crystalline Substrates

Masato M. Maitani[*a§], *Keita Tanaka*[a], *Hirokazu Satou,*[a] *Takayoshi Oshima,*[a§§] *Akira Ohtomo*[a], *and Yuji Wada*[*a]

[a] *School of Materials and Chemical Technology, Tokyo Institute of Technology, 2-12-1 Ookayama, Meguro, Tokyo 152-8552, Japan.*
E-mail: mmaitani@apc.titech.ac.jp; yuji-w@apc.titech.ac.jp
[§] *Research Center for Advanced Science and Technology, The University of Tokyo, 4-6-1 Komaba, Meguro, Tokyo 153-8904, Japan.*
[§§] *Department of Electrical and Electronic Engineering, Saga University, Saga 840-8502, Japan.*

S1 Facet Control of TiO_2 Nano-sheets

Synthesis of TiO_2 Nano-sheets on FTO. The hydrothermal synthesis of anatase TiO_2 nano-sheets exposing the dominant {001} facet was applied to FTO substrates based on the reported process [1]. The direct growth of anatase TiO_2 nano-sheets was performed with a TiO_2 precursor solution composed of $HCl_{aq.}$, titanium (IV) tetrabutoxyde [$Ti(OBu)_4$, TBO] and ammonium hexafluorotitanate (IV) [$(NH_4)_2TiF_6$, ATF], in which a piece of the clean FTO substrate was placed in a Teflon autoclave, and then heated under a microwave irradiation with temperature controlling system utilizing optical probe thermometer. Each sample of TiO_2 was earned after sonication in ethanol for cleaning. Scanning electron microscope (SEM) images (Figure S1-1 a and b) showed TiO_2 nano-sheets that had grown uniformly and were largely tilted with rondom orientations (Figure S1-1 e) from the surface plane of the FTO substrate. The crystalline orientation was examined by high-resolution transmission electron microscope (HR-TEM) with selected area electron diffraction (SAED) in TEM (Figure S1-1 d and c, respectively), and it was confirmed that the large fraction of {001} facet plane was exposed at two sides of decahedral anatase crystals as generally expected [2-6]. The lattice structure observed on the square plane of nano-sheets also supports the predominance of the {001} plane, revealing the atomic separation of 0.19 nm that can be attributed to the atomic distance in the [200] direction of anatase TiO_2. SAED results also showed the diffraction pattern associated with the {001} facet of anatase TiO_2 crystals. The inter-planar angle of 68.3° between the {101} and {001} facets was also observed in SEM images, as reported previously[2-6].

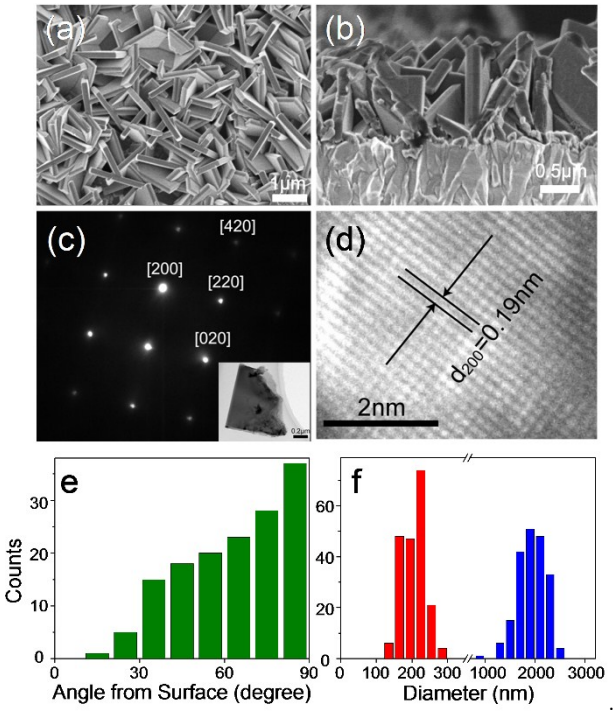

Figure S1-1 FE-SEM images of (a) plane and (b) crossection and (c) SAED of TEM and (d) HR-TEM images of synthesized TiO_2 film exposing {001} facet of anatase TiO_2 on FTO substrate. The TEM images were taken on the square (001) plane of cleaved TiO_2 nanosheet as indicated in the inset of c. The distributions of (e) angle of {001} facets with respect to the surface plane of FTO and (f) diameter of TiO_2 crystals in a- and c-axis are summarized by analysis of more than 100 particles in SEM images

The fraction of exposed {001} facet of precipitated TiO_2 was also determined to be ≈75% by the diameters in the a- and c-axes (Figure S1-1 f) based on the assumption of ideal anatase being crystalline with a decahedral shape(Figure S1-2). Based on the ideal structure of anatase TiO_2 particle indicated in Figure S1-2 [2-6], we determined the geometric values of synthesized TiO_2 nano--particles from mean values of *a* and *c* measured in SEM and TEM images. According to the assumption that the interplanar angle between the (101) and (001) faces equals 68.3 degrees, we calculated values of d and L geometrically and summed surface areas of {001} and {101} facets, $S_{(001)}$ and $S_{(101)}$, respectively (Figure S1-2). The fraction of {001} facets was determined from $S_{(001)} / S_{total}$.

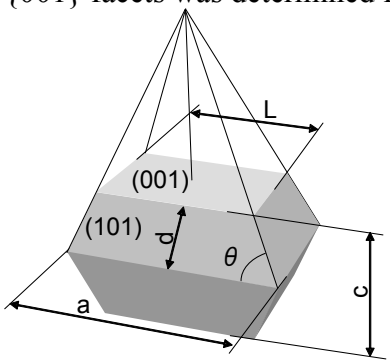

$$d = \frac{c/2}{\sin(68.3°)} \quad \text{(S1)}$$

$$L = a - \frac{2 \times (c/2) \times \cos(68.3°)}{\sin(68.3°)} \quad \text{(S2)}$$

$$S_{(001)} = 2 \times L \times L \quad \text{(S3)}$$

$$S_{(101)} = 6 \times (a + L) \times d / 2 \quad \text{(S4)}$$

Figure S1-2. The modeled anatase TiO_2 nanparticle structure used for the calculations of geometrical characteristics.

XRD revealed peaks attributed to the anatase crystal in addition to peaks from the FTO substrate (Figure S1-3) ensuring that the anatase TiO_2 particles were prepared on FTO, while detailed analyses of XRD is further discussed later. The results of synthesis without either ATF or TBO proved that anatase TiO_2 sheet growth requires both ATF and TBO (Figure S1-3). In addition, decreasing the concentration of either ATF or TBO degrades the coverage of TiO_2 on the FTO substrate. The molar ratio of F/Ti in the precursor solution was found to be optimized at a value of 2.8.

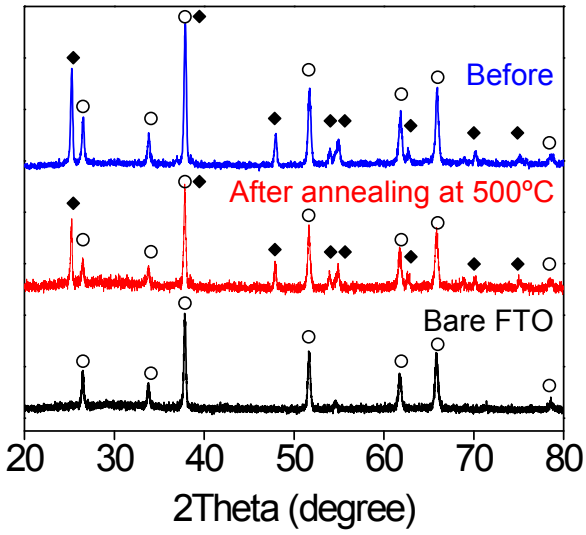

Figure S1-3. Out-plane XRD of TiO_2 naosheets grown on FTO indicated in Figure 1 before (blue) and after (red) aneealing at 500 ºC, with reference spectrum of bare FTO marked with FTO (circle) and anatase TiO_2 (diamond) peaks.

Aspect Ratio Control of TiO_2 Nano-sheets on FTO. The internal surface area, denoted as RF (i.e. ratio of internal surface area to objective area), is important for electric, optoelectric, and catalytic applications of TiO_2 nano-porous films, such as DSSC. The quantification of the internal surface area was performed with the SEM images for determining the diameter in *a* and *c*-axis of each nanosheets resulting in the averaged surface area of each particle. The internal surface area was calculated from the product of number density on the specific objective area with the averaged surface area of each particle. Since a few conditions of TiO_2 synthesis resulted in ununiformed coverage of TiO_2 crystals on FTO substrates, the averaged coverage determined by the low magnification images of SEM was also considered into the estimation of internal surface area; *i.e.* the coverage is explained (Figure S1-3).

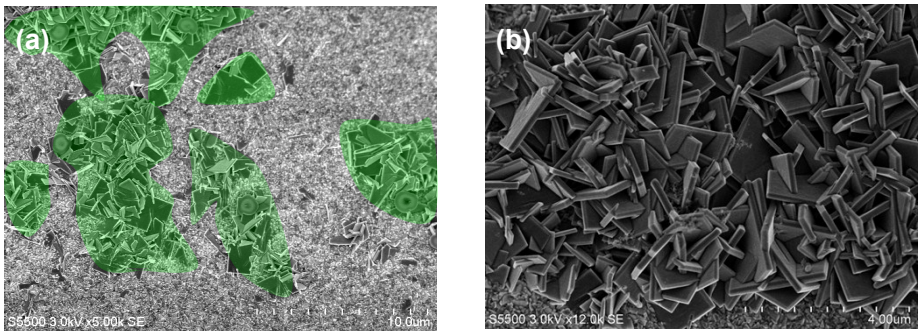

Figure S1-3. SEM images of typical TiO_2 nanosheets on FTO under (a) low magnification and (b) high magnification in the green area. The green area indicates the TiO_2 crystals covering the FTO substrate for defining the TiO_2 coverage (green area vs. total area) on FTO. The population of TiO_2 nanosheets was also counted in specific area in SEM images under the high magnification.

The {001} facet-dominant directly grown TiO_2 nano-sheets on FTO appeared with a relatively low RF of ≈11 as compared with that of conventional nano-porous TiO_2 films composed of nano-particles, which exhibit a typical RF of ≈100 with a one micron thick film. We therefore provide a synthetic strategy to increase the internal surface area of the {001} facet-dominant directly grown TiO_2 nano-sheets by increasing the fraction of the {001} facet, TiO_2 coverage, and population of TiO_2 nano-sheets on FTO substrate. It has been established that the fraction of {001} facet can be increased with addition of fluoride compounds—typically HF—in the hydrothermal processing solution, due to the stabilization of the reactive {001} facet of anatase TiO_2 by fluorination [2-6]. We have trialed the addition of several less-corrosive fluoride compounds to FTO and glass substrates in the precursor solution of TiO_2 for the hydrothermal growth process. Among trials (Figure S1-4), anionic liquids (e.g. $BMImBF_4$) successfully exhibited the ability to increase the fraction of preferred {001} facet, probably due to fluorination of the TiO_2 surface.

Because controlled experiments using 1-butyl-3-methylimidazorium hexafluorophosphate ($BMImPF_6$), KBF_4, and $NaBF_4$ additives did not show any increased {001} fraction, we concluded that the combination of BMIm cations and BF_4 anions collaboratively contributes to the stabilization of the reactive {001} facet. This could be attributed to the mechanism of the collaborational effect of BF_4 and BMIm on the stabilization of the reactive {001} facet, which has not been discussed in previous literature reporting the stabilization of {001} facet with BF_4 during synthesis [7, 8]. Although the collaborational effect of $BMImBF_4$ is not clearly understood, the effect could be related to the adsorption process of imidazolium cations on TiO_2, which could be adsorbed differently on different facets of anatase TiO_2 {101} [9].

Next, we varied the concentration of $BMImBF_4$ in the precursor solution for the hydrothermal growth of TiO_2 nano-sheets and evaluated the resulting fraction of the {001} facet and TiO_2 coverage as a function of the molar fraction of fluorine against titanium (i.e. the F/Ti fraction) in the precursor solutions. Figure S1-4a shows the fraction of {001} facets and RF of TiO_2 film on FTO with a variation of the molar ratio of F/Ti. Each set of synthesis conditions is shown in Table S1. The original optimized condition without the $BMImBF_4$ additive is also indicated at F/Ti of 2.8 in the same plot (series 4). As the amount of added $BMImBF_4$—and thus the F/Ti ratio—was increased, the {001} facet became more dominant and therefore the aspect ratio of each particle was increased with the maximum {001} fraction of 87% at F/Ti of 10 (series 1). This is probably because the higher fluoride concentration stabilized the reactive {001} facet more due to fluorination of 5-coordinate Ti on the {001} facet [2]. According to previous reports, adsorption of BF_4 anions on the TiO_2 surface reduces the surface energy of the reactive {001} facet that has intrinsically high surface energy [7, 8]. Since the growth in the *a*-axis is more rapid than that in the *c*-axis in the original optimized condition without $BMImBF_4$, a shorter synthesis time favored the formation of thinner TiO_2 nano-sheets with more {001} facet. On the other hand, shorter synthesis time also resulted in less coverage of TiO_2 sheets on the FTO substrates, and therefore the longer synthesis time resulted in higher RF due to the larger converge of TiO_2 crystals on FTO substrate (Figure S1-4), as can be seen in the comparison of series 1 and 4 without $BMImBF_4$ addition. The definition of coverage is the projective coverage of TiO_2 on FTO based on the observation with SEM plane view, as shown with the island-like TiO_2 nano-sheets indicated in Figure S1-3. While the addition of $BMImBF_4$ resulted in an increase in the {001} fraction, this was accompanied by a degradation in the coverage of TiO_2 on FTO (Figure S1-4). Therefore, the overall RF of TiO_2 films is limited in series 1, although the aspect ratio of particles was increased as the result of the enlargement of {001} facet fraction. This loss of coverage by addition of $BMImBF_4$ may be related to the adsorption properties of BMIm cations onto the oxide surface (in this case, FTO) [9].

In order to increase the coverage, we optimized the synthesis conditions with a fixed F/Ti ratio of 10.1. Firstly, the concentrations of Ti precursors, $(NH_4)_2TiF_6$ and $Ti(OBu)_4$, were

increased by a factor of 2 under same synthesis conditions as series 1. This dramatically improved the coverage (Figure S1-4), while the surface thus produced exhibited excessive TiO_2 crystal population density with insufficient intercrystalline spacing, resulting in a lower fraction of exposed {001} facet. Therefore, the reaction temperature was reduced to 195°C and 180°C in addition to the aforementioned increase in the concentration of Ti precursors. Under these conditions, TiO_2 nano-sheets were successfully grown with adequate spacing and with a large {001} fraction (series 2), while the population of TiO_2 nano-sheets was also decreased, although the uniformity of TiO_2 particle distribution on FTO was dramatically improved as compared with the series 1.

To increase the population of TiO_2 on FTO, the synthesis time was extended to 3h, and we thus successfully obtained the TiO_2 nano-sheets densely populated uniformly across the FTO substrate with large (up to 88%) fraction of {001} facet (series 2 in Figure 1-4). Finally, increase in RF of TiO_2 films of more than 100% was achieved by exposing more than 88% of {001} facet fraction of directly grown TiO_2 nano-sheets on FTO substrate with addition of $BMImBF_4$ additive (Figure S1-4). We additionally applied the higher concentration of $BMImBF_4$ with an F/Ti ratio of ≈18 and achieved more than 90% {001} fraction (series 5), although the RF was not dramatically increased due to the limited coverage. Therefore, we proved one of the strategies to increase the fraction of {001} facet by adding the fluoride compound, $BMImBF_4$, stabilizing the {001} facet of anatase TiO_2 in order to expand the RF of 22 with {001} facet-dominant TiO_2 nano-sheets grown on FTO.

Table 1. Synthetic conditions of each series in Figure 2.

	TBO (molar fraction)	AFT (molar fraction)	$BMImBF_4$ (molar fraction)	Temp. (°C)	Synthesis Time (min)
Series 1	1	1.2	0~4	210	60
Series 2	2	2.4	8	180	60
Series 3	2	2.4	8	180	180
Series 4	1	1.2	0	210	75
Series 5	1	1.2	8	210	240

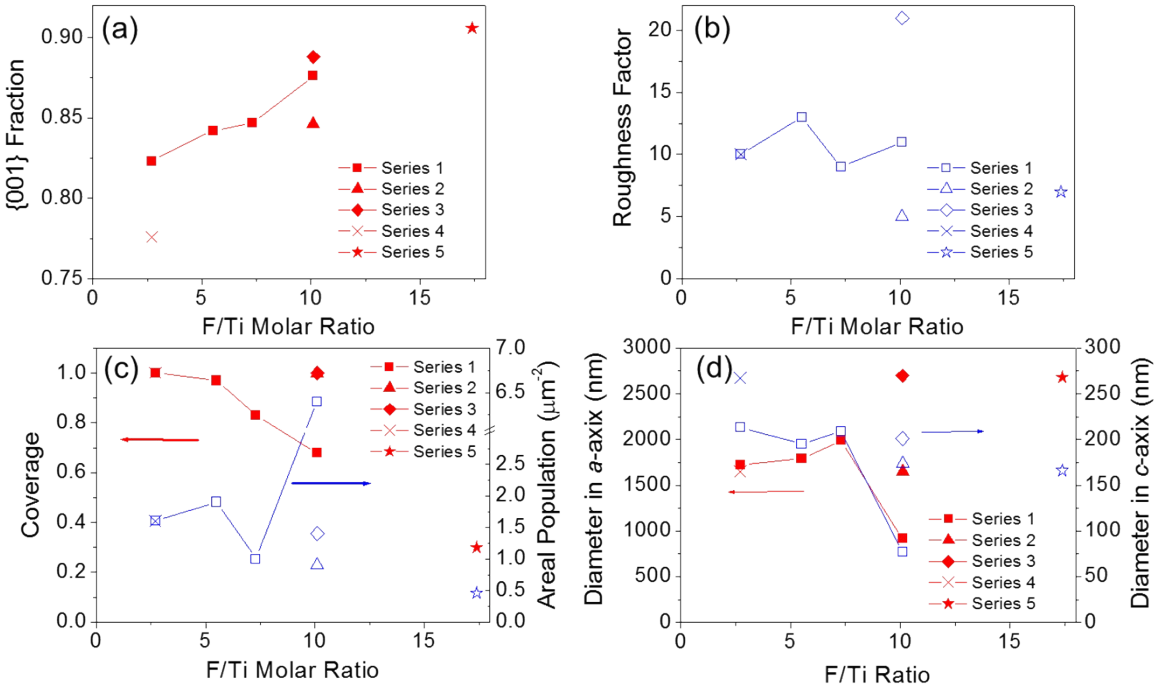

Figure 1-4. (a) The facet fraction determined by SEM observation and (b) corresponding RF calculated by the TiO_2 coverage and TiO_2 nanosheets areal population with averaged surface area of each nanosheets over the projection area. (c) Coverage and areal population and (d) diameter in *a*- and *c*-axis of anatase TiO_2 nanosheets determined by SEM observation.

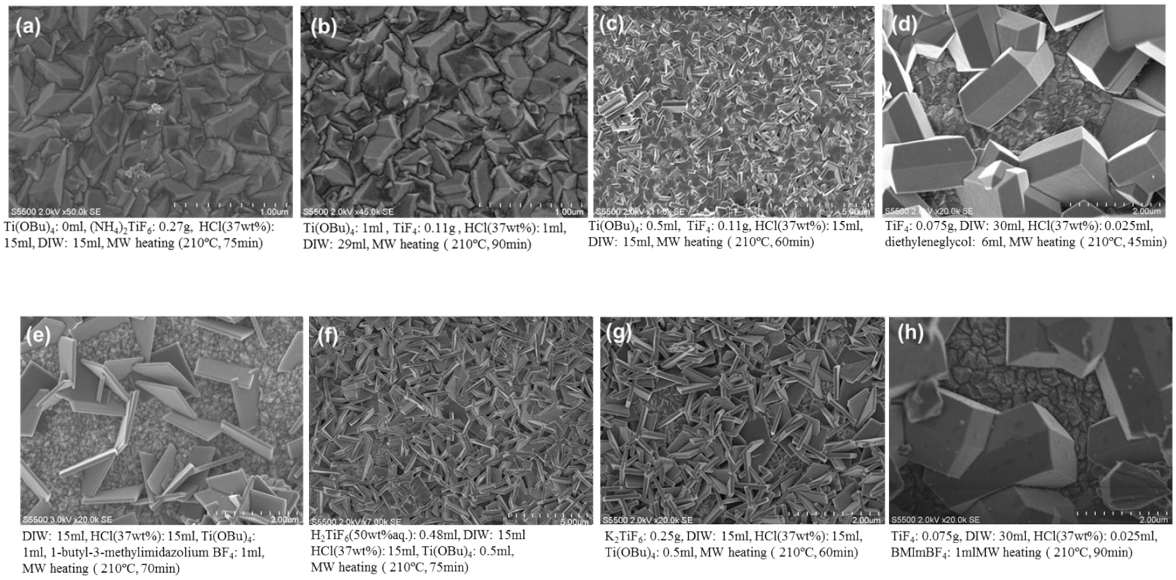

Figure S1-5. SEM images of TiO_2 naosheets grown on FTO with addition of several kinds of additives in order to increase {001} facet of anatase TiO_2 as conditions are indicated as the captions.

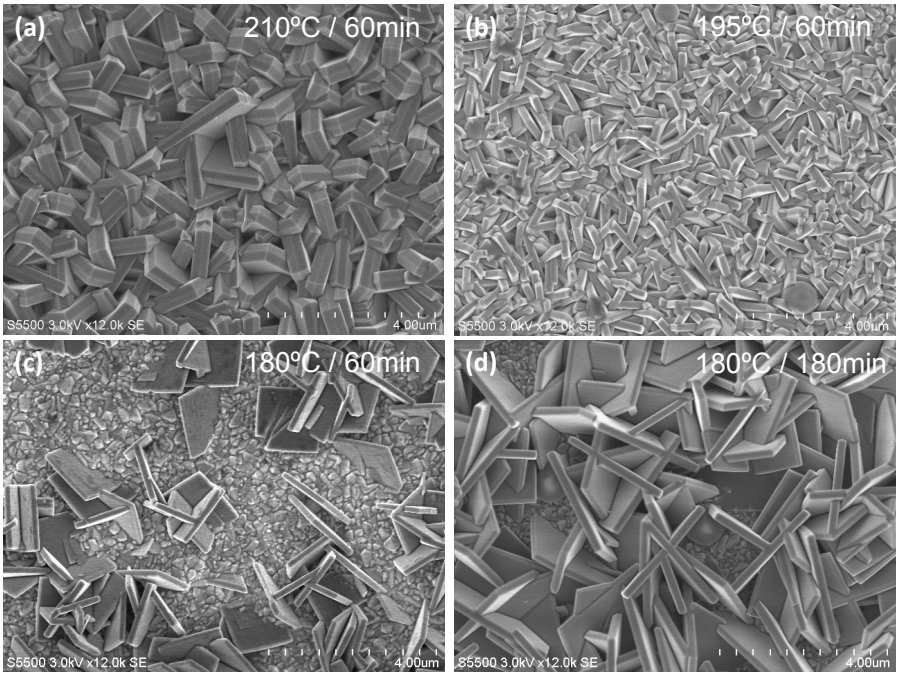

Figure S1-6 SEM images ofTiO_2 nanosheets on FTO in the condition of (a) 210 ºC, (b) 195 ºC, and (c) 180 ºC for 60min and (d) 180 ºC for 180min.

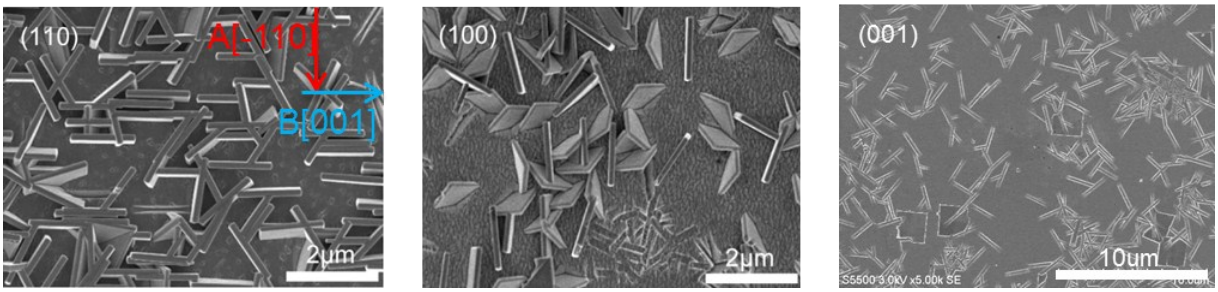

Figure S2-1. SEM images of TiO_2 nanosheets on rutile TiO_2 exposing (110), (100), and (001) plane views.

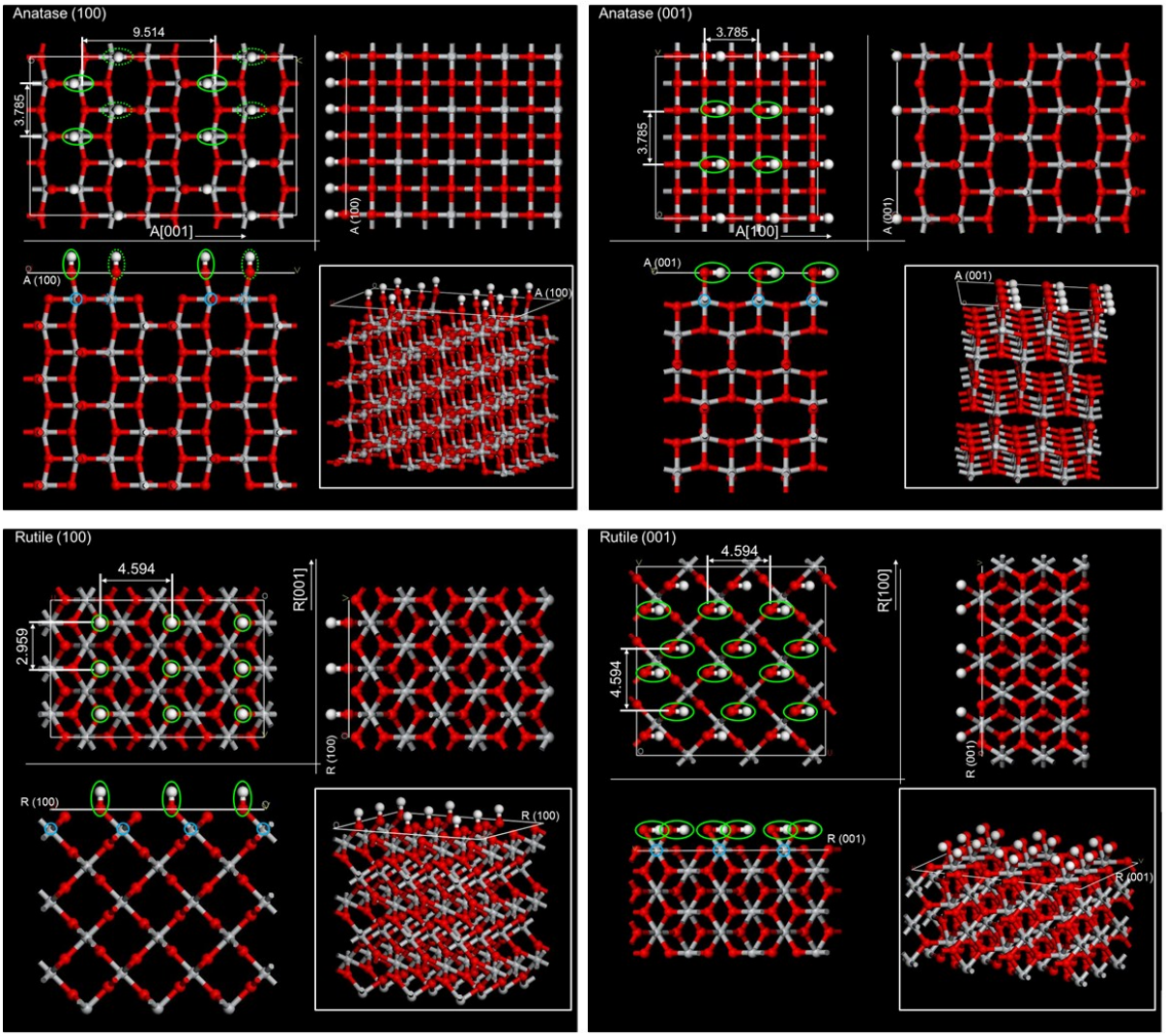

Figure S2-2. Crystallographic images of anatase (top) and rutile (bottom) TiO_2 surface with (100) and (001) facets with plane (left top), crossection (right top and left bottom), and side (right bottom) views[2-9].

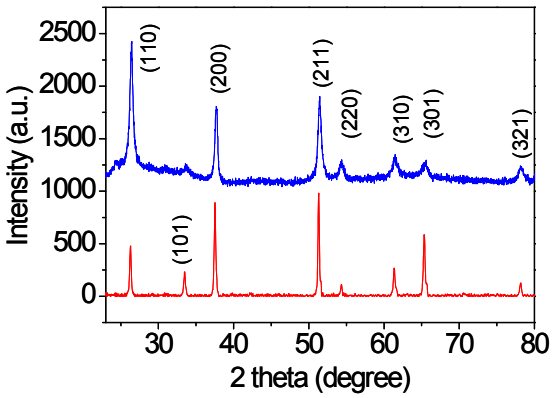

Figure S3. Out-plane XRD of flat well-aligned poly-crystalline SnO_2 (blue) and randomly-aligned poly-crystalline SnO_2 of FTO (red) on glass.

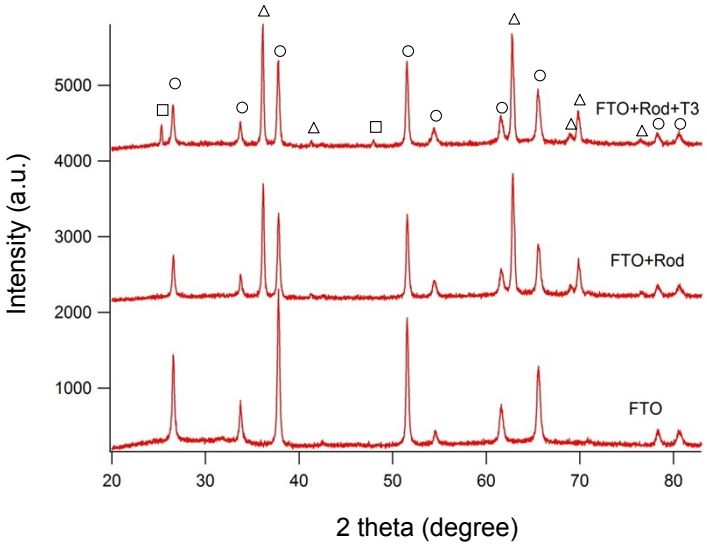

Figure S4. XRD of hierarchical antase TiO_2 nanosheets on rutile TiO_2 nanowires with reference FTO substrate and primary rutile TiO_2 nanowires on FTO. Each peak is assigned to either anatase TiO_2 (square), rutile TiO_2 (triangle), and rutile SnO_2(circle).

Reference

(1) Feng, S.; Yang, J.; Zhu, H.; Liu, M.; Zhang, J.; Wu, J.; Wan, J. Synthesis of single crystalline anatase TiO2 (001) tetragonal nanosheet-array films on fluorine-doped tin oxide substrate. *J. Am. Ceram. Soc.* **2011**, *94*, 310.

(2) Yang, H. G.; Sun, H. S. Qiao, S. Z.; Zou, J.; Liu, G.; Smith, S. C.; Cheng, H. M.; Lu, G. Q. Anatase TiO2 single crystals with a large percentage of reactive facets. *Nature* **2008**, *453*, 638.

(3) Han, X.; Kuang, Q. Jin, M.; Xie, Z.; Zheng, L. Synthesis of Titania Nanosheets with a High Percentage of Exposed (001) Facets and Related Photocatalytic Properties. *J. Am. Chem. Soc.* **2009**, *131*, 3152

(4) Sun, C. H.; Yang, X. H.; Chen, J. S.; Li, Z.; Lou, X. W.; Li, C.; Smith, S. C.; Lu, G. Q.; Yang, H. G. Higher charge/discharge rates of lithium-ions across engineered TiO2 surfaces leads to enhanced battery performance. *Chem. Commun.* **2010**, *46*, 6129

(5) Liu, M.; Piao, L.; Ju, S.; Yan, X.; He, T.; Zhou, C.; Wang, W. Anatase TiO2 single crystals with exposed {001} and {110} facets: facile synthesis and enhanced photocatalysis. *Chem. Commun.* **2010**, *46*, 1664.

(6) Liu, S.; Yu, J.; Jaroniec, M. Tunable Photocatalytic Selectivity of Hollow TiO2 Microspheres Composed of Anatase Polyhedra with Exposed {001} Facets. *J. Am. Chem. Soc.* **2010**, *132*, 11914.

(7) Zhang, D.; Li, G.; Wang, H.; Chan, K. M.; Yu, J. C. Biocompatible anatase single-crystal photocatalysts with tunable percentage of reactive facets. *Cryst. Growth Des.* **2010**, *10*, 1130;

(8) Zhang, D.; Li, G.; Yang, X.; Yu, J. C. A micrometer-size TiO2 single-crystal photocatalyst with remarkable 80% level of reactive facets. *Chem. Commun.*, **2009**, 4381.

(9) Burdett,J. K.; Hughbanks, T.; Miller, G. J.; Richardson, Jr. J. W.; Smith, J. V., Structural-Electronic Relationships in Inorganic Solids: Powder Neutron Diffraction Studies of the Rutile and Anatase Polymorphs of Titanium Dioxide at 15 and 295 K, *J. Am. Chem. Soc.* **1987**, *109*, 3639-3646.